

Case study: Figurines Holy Family (Art & History Museum, European ethnology collection, Brussels)

Case study image:



Authors of the report: Marina Van Bos, Ina Vanden Berghe, Maaïke Vandorpe (Labs KIK-IRPA)

Report date: November 18, 2021

1. Non-invasive analysis

1.1. Methodology

XRF

For the material-technical analyses of the figures of the holy family, X-ray fluorescence (XRF) analyses were performed. Despite a number of limitations and drawbacks, mobile XRF has been successfully used in the past for the identification of pigments in murals, manuscripts, etc.

XRF is an elemental analysis technique that makes it possible to identify the chemical elements present within the irradiated zone, without taking into account the stratigraphy. The chemical elements can thus be present both in the surface layer and / or in the underlying layer(s) (this depends on the nature of the chemical elements and the thickness of the layers).

A second disadvantage of the technique is that the information obtained is “elementary” information and not molecular information. For example, when lead is detected in a paint layer, this may indicate the white pigment lead white [$2 \text{PbCO}_3 \cdot \text{Pb}(\text{OH})_2$], or the red lead red (minium) [$2\text{PbO} \cdot \text{PbO}_2$], or the yellow massicot [PbO], or a mixture

Light chemical elements are not detected (positive identification from potassium) and organic pigments / binders cannot be identified.

This technique thus provides a general overview of the chemical elements present in the analysed zone.

The XRF technique is based on the following principle: a primary x-ray (coming from the x-ray source in the equipment) is aimed at the paint layer. Secondary X-rays, characteristic of the chemical elements present, are generated. Due to the high energy of the incident primary x-rays, secondary x-rays are generated not only in the surface layer but also in the underlying layer(s). This obviously complicates the interpretation of measurement results.

All measurements were performed with a μ -XRF instrument ARTAX (Bruker) with a rhodium (Rh) tube with polycapillary optics, which gives the primary x-ray beam a diameter of approximately 70 μm , which allows to analyze very fine details (Figure 1) . The measurement location can be accurately selected using a CCD colour camera (figure 2).



Figure 1: XRF measuring equipment

A typical analysis result is presented in Figure 3.

The following experimental conditions were used in all measurements: Rh tube, 50 kV, 500 μA , 120 seconds, no filter.

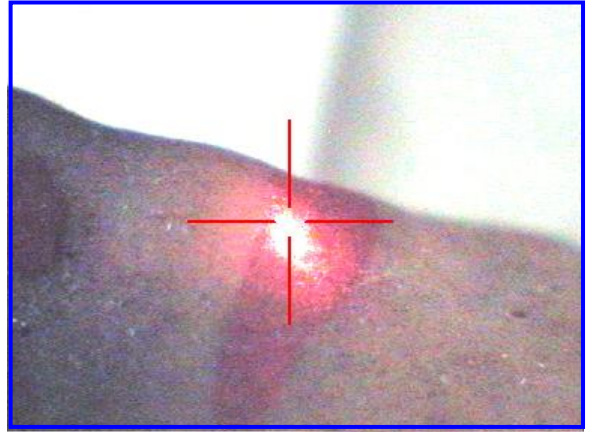


Figure 2: Separate head (left) and image taken by the camera of the XRF equipment (detail lips). The analysed zone (70 μ m) is in the middle of the cross

All images registered by the XRF-camera (visualisation of the measuring spots) are displayed in this report.

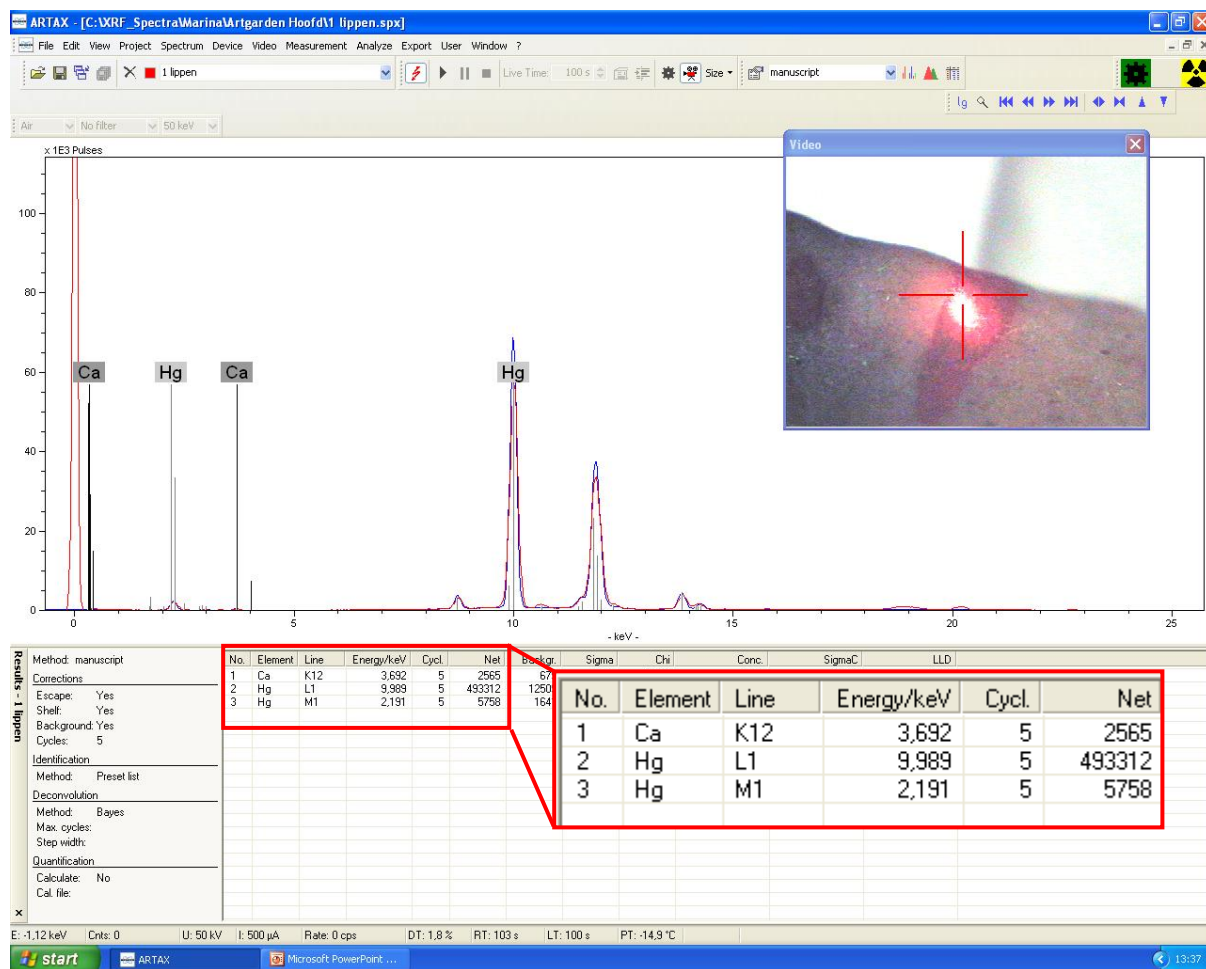


Figure 3: X-ray spectrum and data processing of the analysed spot presented in figure 2 (lips)

The interpretation of the spectrum above gives the following result:

The lips are painted using vermilion. Calcium can be present in the paint layer (as the white pigment chalk) or calcium originates from the support (the head), probably as gypsum (calcium sulphate) (sulphur is not easily detected using our XRF equipment).

As explained, the interpretation of XRF analyses alone is not always unambiguous: only elementary information is obtained and different pigments can at the same time give rise to secondary X-rays. The interpretation is a combination of the obtained element information and, in case of pigments, also on the observed colour. Sometimes multiple interpretations are possible.

A total of 15 measurement points were selected.

All the selected measurement locations are indicated in figure 4 and 5.



Figure 4: The holy family with indication of XRF measuring spots



Figure 5: The separate head with indication of XRF measuring spots

1.2.Results

Hirox digital microscope images are registered at areas corresponding to the XRF analysed areas.



Figure 6: Hirox digital images

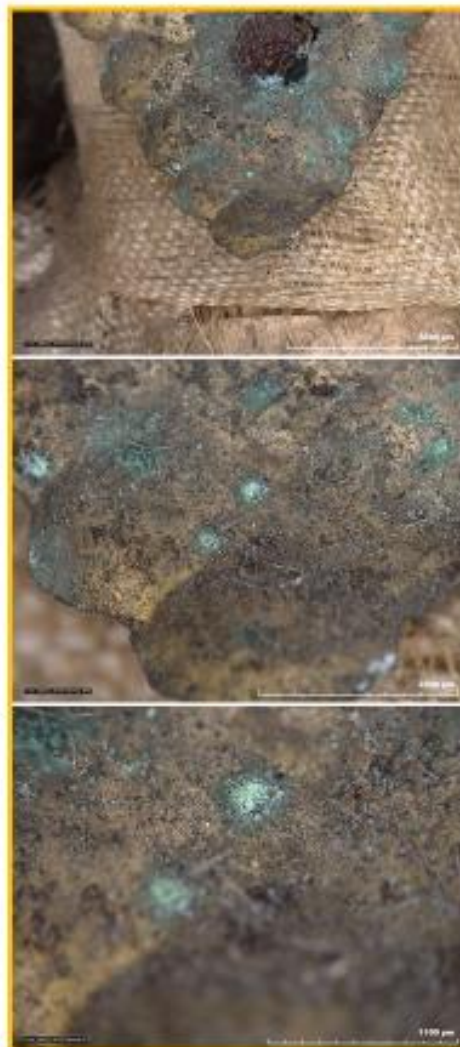


Figure 7: Hirox digital images



Figure 8: Hirox digital images



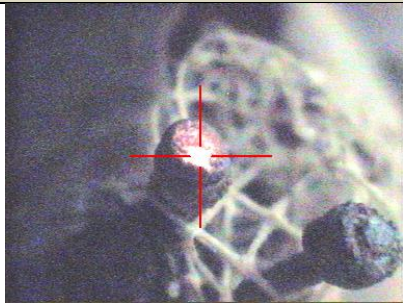
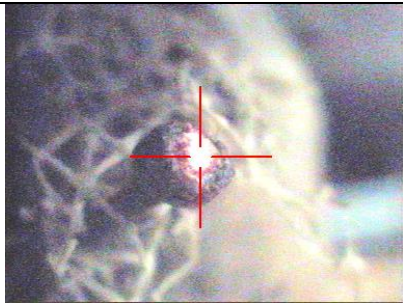
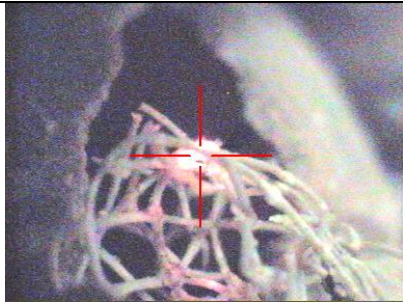
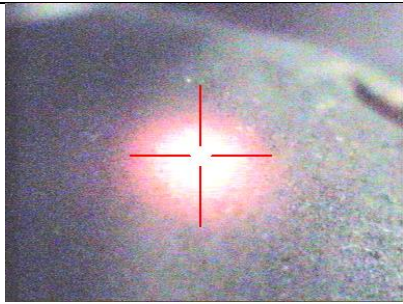
Figure 9: Hirox digital image

back of the head

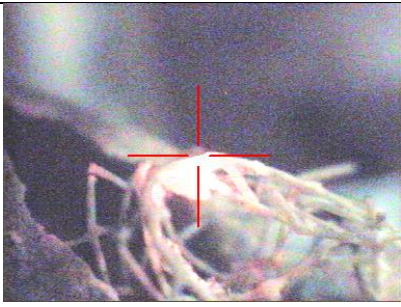
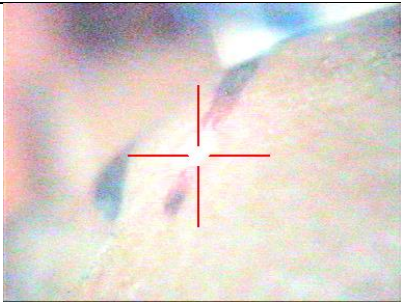
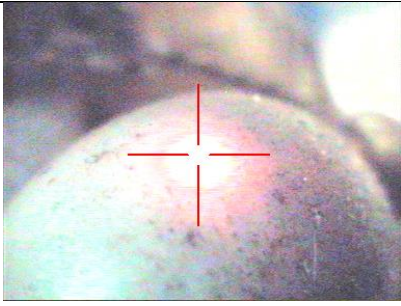
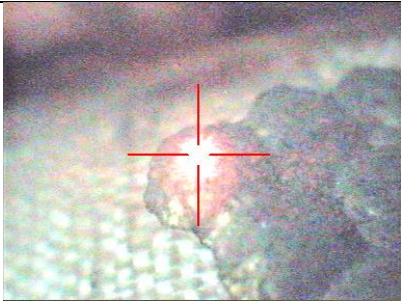
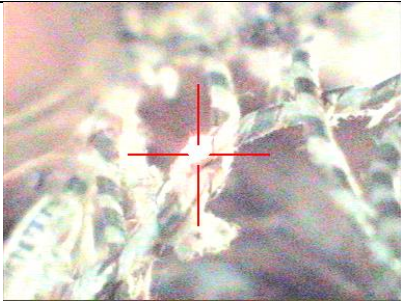
The results of the analyses are summarized in table 1 and 2.

Table 1: description of the analysed zones and results of analyses of the holy family: sulfur (S), potassium (K), calcium (Ca), titanium (Ti), manganese (Mn), iron (Fe), nickel (Ni), copper (Cu), zinc (Zn), strontium (Sr), tin (Sn), barium (Ba), lead (Pb)

Elements present in low concentrations are in parentheses ¹

N°	Measuring place (image Artax-camera)	Description	Results of XRF-analyses	Interpretation
XRF 1		Nail on head	Fe , Ca, (Ti), (Pb), (Cu), (Zn)	Iron metal
XRF 2		Nail on head	Fe, (Sn), (Ca), (Cu)	Iron metal, tin solder in the middle?
XRF 3		Textile on head	Pb, Fe, Ni, Ca, (K), (Ti), (Ba), (Sn), (Mn)	Lead white ?
XRF 4		Head	Ca , Sr, S, (Fe)	Calcium carbonate/ Calcium sulphate

¹ > 100.000 counts in bold, >10.000 in normal letters, >1000 in parentheses

XRF 5		Textile on head	Pb, (Ca), (Fe), (K), (Ni), (Ti), (Ba)	Lead white?
XRF 6		Eyebrow	Ca, S, (Fe)	Calcium carbonate/ Calcium sulphate Carbon based black
XRF 7		White pearl	Pb, (K), (Fe), (Ca)	Lead white?
XRF 8		Leaf	Cu, Zn, Fe, (Ni), (K)	Copper zinc alloy (brass)
XRF 9		Metal wire	Cu, Zn, Fe, (K), (Ca), (Ni)	Copper with minor amount of zinc (brass)

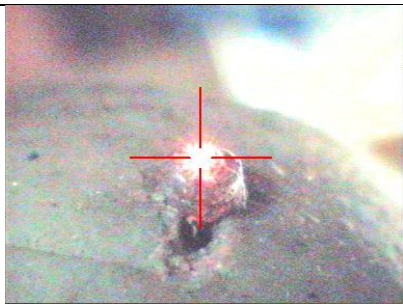
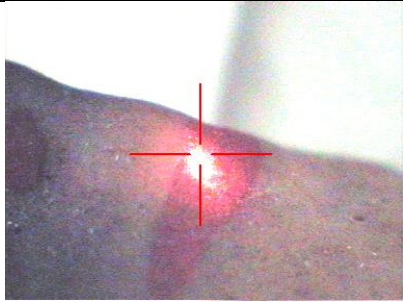
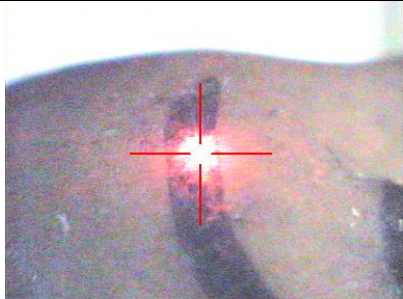
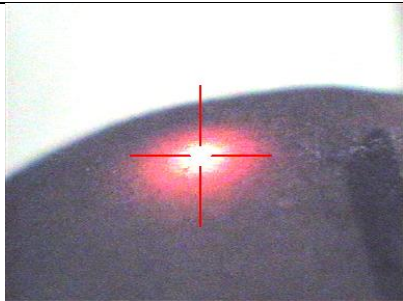
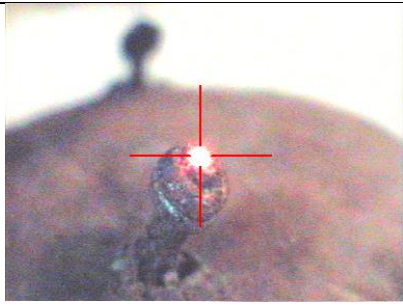
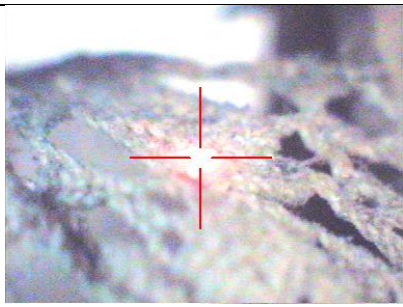
XRF 10		Nail on back of the head	Fe , Sn, Cu, Pb, Zn	Iron metal, tin solder in the middle?
--------	---	--------------------------	----------------------------	---------------------------------------

Table 2: description of the analysed zones and results of analyses of the separate head: sulfur (S), potassium (K), calcium (Ca), iron (Fe), copper (Cu), zinc (Zn), strontium (Sr), tin (Sn), mercury (Hg), lead (Pb)

Elements present in low concentrations are in parentheses ²

N°	Measuring place (image Artax-camera)	Description	Results of XRF-analyses	Interpretation
XRF 1		Lips	Hg , (Ca)	vermilion
XRF 2		Eyebrow	Ca , Sr, S, (Fe)	Calcium carbonate/ Calcium sulphate Carbon based black
XRF 3		Forehead	Ca , Sr, S, (Fe)	Calcium carbonate/ Calcium sulphate

² > 100.000 counts in bold, >10.000 in normal letters, >1000 in parentheses

XRF 4		Nail	Fe, Sn, Cu, Ca, Pb, (Zn)	Iron metal, tin solder in the middle?
XRF 5		Textile	(Fe), (Ca), (K) ?	

2. Invasive analysis

2.1.Head

In addition to these XRF analyses, one small sample (sample size $\approx 1 \text{ mm}^2$) was withdrawn from the inside of the separate head. This sample was analysed by infrared spectroscopy (FT-IR, Hyperion 3000 microscope coupled to a Vertex 70 spectrometer, both from Bruker). The sample was pressed between 2 diamond windows of a SpectraTech compression cell in order to obtain a transparent layer of the material to be analysed. The spectrum was recorded in transmission mode, in the range $4000 - 650 \text{ cm}^{-1}$, with 64 scans and 4 cm^{-1} resolution.

For other objects from the museum's collection and which are also part of the Artgarden project, the figures always have wax heads. The XRF analyses indicated a composition based on calcium sulphate/carbonate.

FT-IR analyses confirmed the presence of calcium sulphate. In addition beeswax was present.

2.2. Textile

Sample Description

Not much is known about the provenance and the conservation history of this object, though it is clear that the figures have suffered very much over time. Parts of the object are lacking, metal decoration is corroded and parts of the costumes have completely disappeared. Three fabrics will be studied, the beige dresses from the left person and the child, and the red/brown striped fragment (shirt) (figure 10).



Figure 10: Two beige dresses and the red shirt with indication of the sample location

Beige dresses

The beige dresses of the left person and child figure are heavily degraded. They are made of very fine silk fabrics that are positioned in direct contact with the basic structures of the figures made of **straw, or with the support made of paper or cardboard**. To better understand the cause of the extensive degradation of these silk fabrics, we take samples to identify the presence of dyes and other substances in the threads.



A fragment of the degraded silk of the adult figure is taken at the bottom of the back side of the figure (figure 10, right). This fragment will be used for dye (/k01) and SEM-EDX analysis (/v01).




A sample of the degraded silk of the child's dress is taken at the frontside (figure 10, left). Again the yarns are used for dye (/k03) and SEM-EDX analysis (/v03).

Red/brown striped fabric (shirt)

The second figure (decapitated person) wears a shirt with vertical red and brown stripes. The textile is composed of brown yarns in horizontal direction and red and brown yarns in vertical direction. An attempt was made to sample both brown and 'red yarns'. However sampling was limited and only the red yarn could be taken (/k02).

Table 3: Overview of the samples with indication of the object, sample description and image, KIK sample code and type of analyses

Object	Sample description	Image + KIK/IRPA code (images©KIK-IRPA Textile Lab)	Analysis / Technique(s)
Beige silk dress person on the left	White and beige yarns	 14426a/k01	Dye identification (HPLC-DAD)
	Strong degraded silk	 14426a/v01	Silk degradation (HPLC-FL, FT-IR, MRS) SEM-EDX OM

Beige silk dress - child	White and beige yarns	 <p>14426a/k03</p>	Dye identification (HPLC-DAD)
	Strong degraded silk	 <p>14426a/v03</p>	Silk degradation (HPLC-FL, FT-IR, MRS) SEM-EDX OM
Red/brown striped fabric	Red/white yarn <i>Only the red part was taken for analysis</i>	 <p>14426c/k02</p>	Dye identification (HPLC-DAD)

2.2.1. Methodology

HPLC-DAD

The identification of the organic colorants is performed by High Performance Liquid Chromatography and photo diode array detection system (HPLC-DAD) with Alliance HPLC equipment (Waters, USA). The analyses are interpreted using the Empower software system from Waters. A detailed description of the analytical protocol was published before (Vanden Berghe et al. 2009). The colorants are recovered from the fibres using acidic extraction with hydrochloric acid (HCl). Hydrochloric acid extraction was preferred to extract the dyes, as to identify a very wide range of organic dyes, either natural or (half) synthetic, by comparison with spectra from the in-house developed textile colorant reference database. An additional analysis was conducted with dimethylsulfoxide (DMSO). Preliminary to the analysis, the samples are examined under binocular in order to avoid any visible surface contamination.

The result of the HPLC-DAD analyses of the extract is listed in Table 4. The first column comprises the code of the sample given by KIK-IRPA, followed by the sample colour in the next column. The type of extract analysed and the analysis code are mentioned in the third and fourth columns. The results of the chromatographic analyses are given in the following two columns. The dye composition mentioned in column five is expressed as relative proportions of the dye constituents after calculation of their peak area measured at the wavelength (nm) mentioned in column six.

Fibre

Fibre identification is carried out with optical microscopy under transmitted or polarizing illumination (OM, Axiomager M1, Zeiss). For this, a few fibres are taken from each sample. Prior to the analysis, the sample is examined under reflective light using the digital microscope KH 8700 from Hirox.

The identification of the fibres is carried out on the basis of the fibre morphology in longitudinal view. Vegetable fibres are identified by their diameter and the presence of characteristic properties (1967; Von Bergen and Krauss 1945). Animal fibre are characterized on the basis of their diameter, the presence of a cuticle with specification of the scales, the cortex (pigmented or not) and the presence or absence of a medulla and the type (Petraco and Kubic 2004). If relevant, the medullary index is also determined, based on of which a distinction can be made between hair of animal and human origin (Kshirsagar et al. 2009).

The morphology of the fibres is then compared with that of reference fibres derived from published atlases (1967; Von Bergen and Krauss, 1945), online atlases and / or the internal KIK database (Vanden Berghe).

Identification between the different bast fibres is based on their differences in fibrillar orientation. This test is known as the modified Herzog or red plate test (Petraco & Kubic 2004; Haugan 2013).

SEM-EDX

The elementary composition is studied by SEM-EDX (scanning electron microscopy coupled with energy dispersion X-ray spectroscopy, Zeiss EVO LS15 and detector of Oxford Instruments). Prior to analysis the samples were coated with a thin layer of carbon. The secondary electron images of the samples with indication of the analysed zones, as well as the corresponding spectra are given.

2.2.2. Results

Red/brown striped fabric (shirt)



Figure 11: Hirox images of the striped fabric red/brown fabric

Hirox images show that the red yarns are made by partially red and uncoloured yarns (Figure 11). Only the red yarns are taken for dye identification.

Carminic acid is the main dye compound detected in the red sample (/k02). This anthraquinone dye constituent refers to the use of the scale insect cochineal. Recalculation of the detected compounds results in the identification of the Mexican cochineal species (*Dactylopius coccus* Costa) (Vanden Berghe, 2016). Furthermore, tannins were used as weighting and mordant agent (table 2).

Table 4: Result HPLC-DAD analyses. Detected dye composition

KIK/IRPA code	Colour	Extr.	Analysis n°	Dye composition	λ (nm)
14426a/k02	Red	HCl	02/210208/06	2 mphb, 1 flavokermesic -C-glycoside, 53 carminic acid, 39 ellagic acid, 2 carminic acid', 1 carminic acid'', 1 flavokermesic acid, + kermesic acid	255
				1 flavokermesic -C-glycoside, 97 carminic acid, 2 flavokermesic acid + kermesic acid	R275

Beige dresses

The extensive degradation of the silk fabrics was initially documented with high resolution Hirox images (figure 12). It is clear that a large part of the fragments is completely gone. A few detached remains are still found at the bottom of the object, but most have already been removed. From the holes in the remaining fabrics we can see that these were caused by the breaking off of threads in both the warp and weft directions (see detail in blue). In other places, it is clear that it is mainly the thicker silk threads without torsion that are the first to break and disappear (see detail in yellow).

These degraded silk fragments are in great contrast to some other areas with much better preserved silk, as from the shawl of the decapitated figure (figure 13, see detail in green).



Figure 12: Hirox images showing details of the extensive degraded silk fabrics



Figure 13: Hirox images of an area of much better preserved silk from the shawl of the decapitated figure

The fragile white/beige silk fabrics used for the child and the adult figure on the left side are compared. Figure 14 shows that they are both made of very fine beige silk warp threads and wider, white weft threads consisting of untwisted silk filaments.

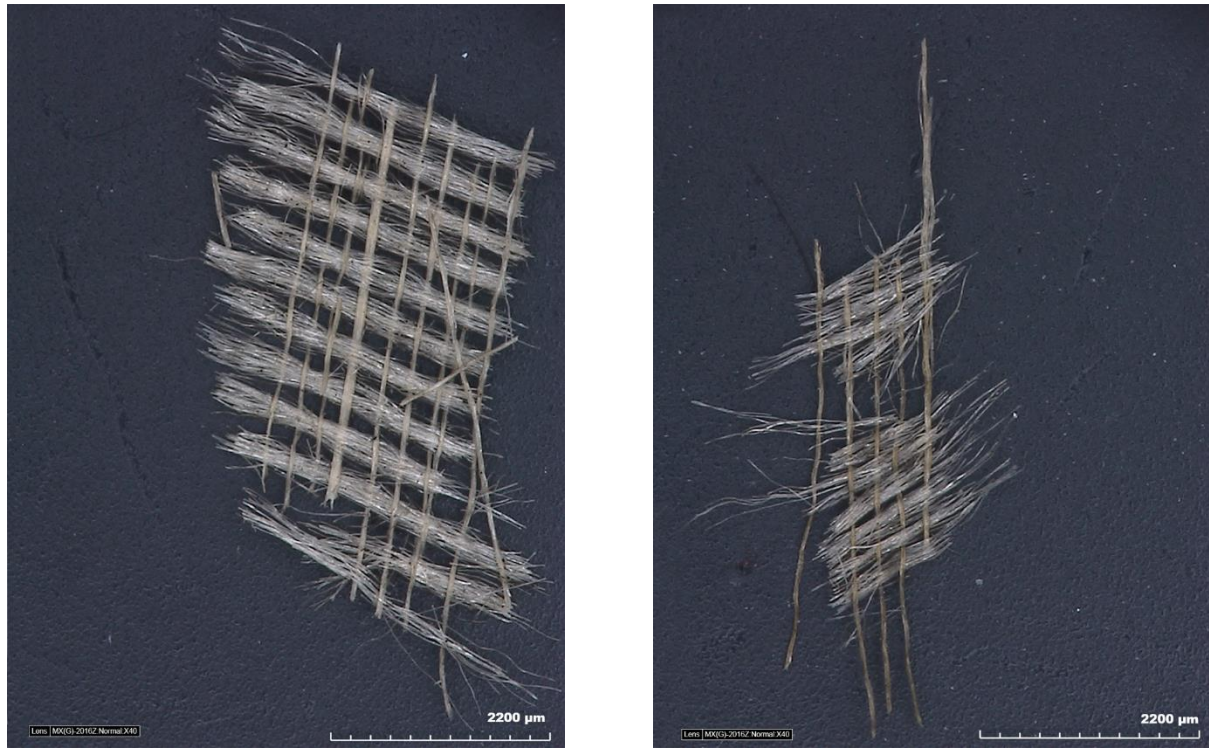


Figure 14: structure of the silk fragments taken from the male's (left) and the child's dress (right)

Both white and beige yarns of the silk of the adults dress are analysed separately. The samples are very small and brittle, though both yarns are identified as degummed cultivated silk *Bombyx mori* L. (figures 15-16).

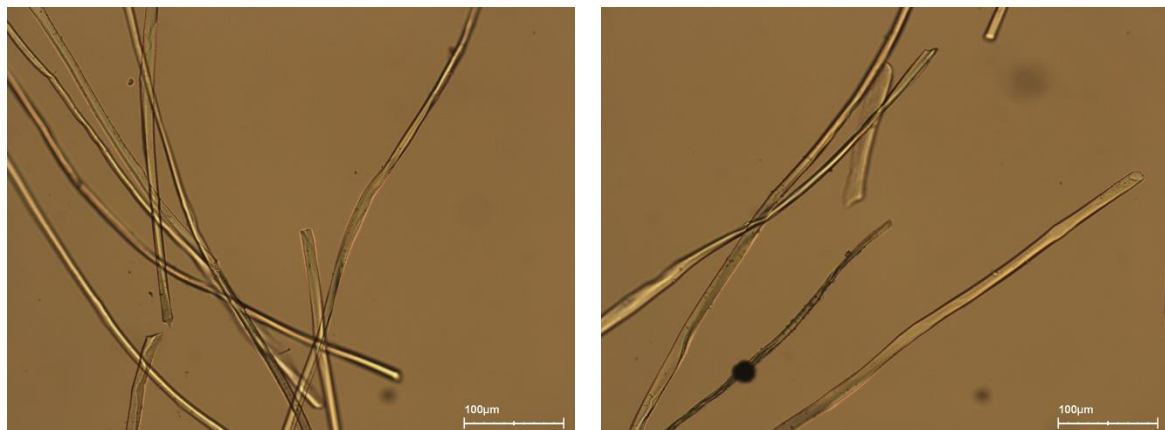


Figure 15: microscopic images with transmission light of the white yarns of sample 14426a/v01 (magnification 200x)

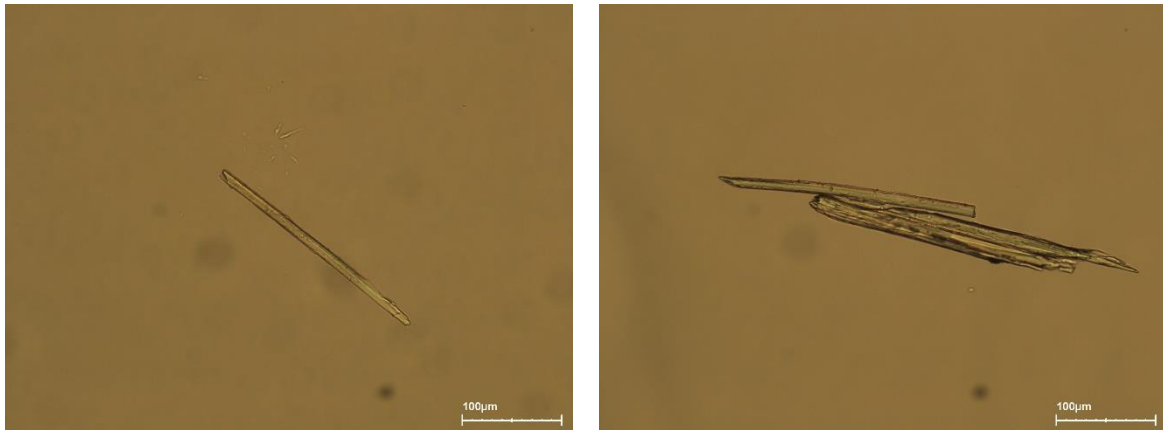


Figure 16: microscopic images with transmission light of the beige yarns of sample 14426a/v01 (magnification 200x)

No dyes are detected in the two silk samples of the dresses (/k01 and /k03) from which we can conclude that these silks were undyed.

Table 5: Result HPLC-DAD analyses. Detected dye composition

KIK/IRPA code	Colour	Extr.	Analysis n°	Dye composition	λ (nm)
14426a/k01	White + beige	HCl	02/210208/05	58 phb, 42 pmb /	255 314
		DMSO	02/210318/04	92 phb, 8 pca /	255 314
14426a/k03	White + beige	HCl	02/210208/07	63 phb, 37 pmb /	255 314

The pronounced degradation of the filaments in both directions of the silk fragments is clearly visible on the secondary electron images, with many broken filaments in the yarns of both directions.

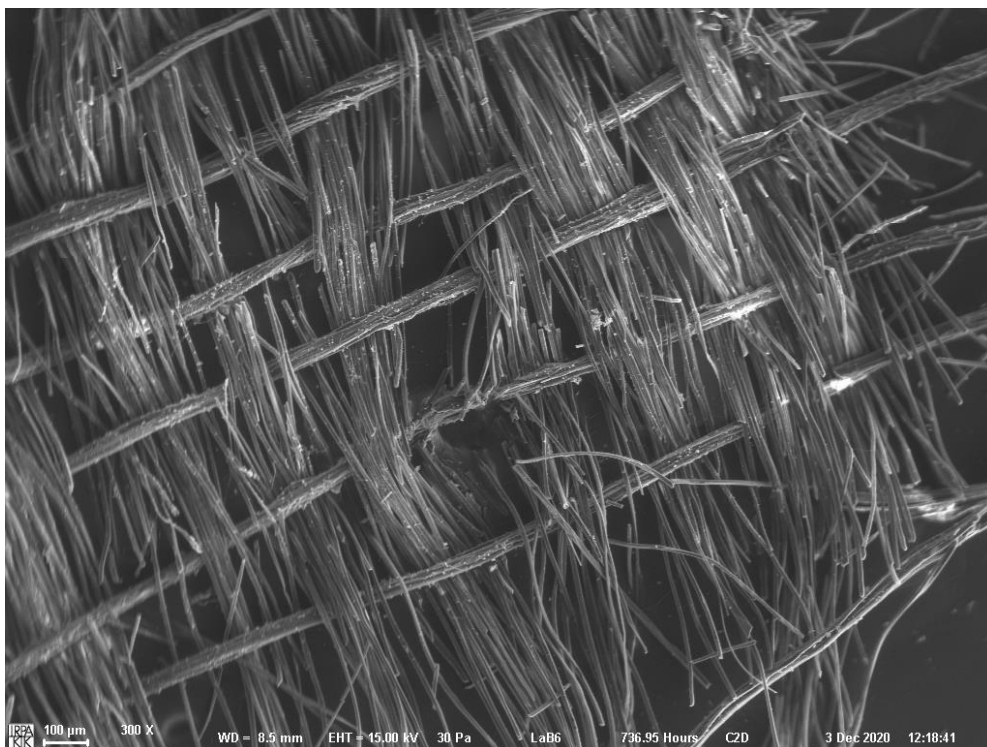
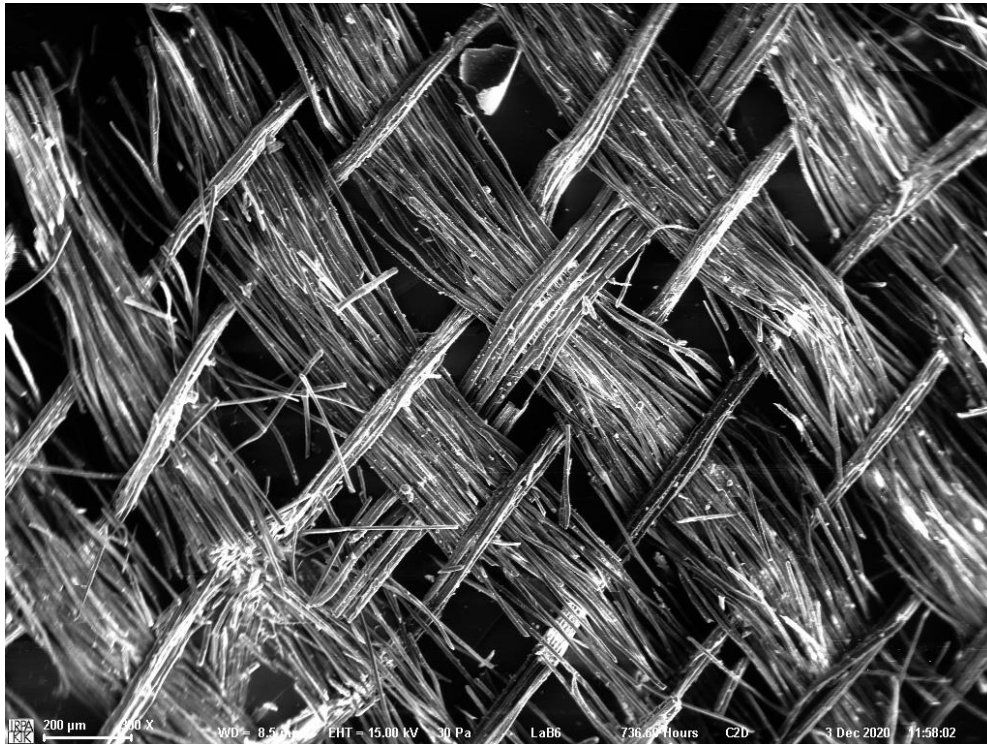


Figure 17: secondary electron images of the silk fabrics from the dress of the male, sample 14426a/v01 (top) and the child, sample 14426a/v03 (bottom)

In addition, the backscattered electron images indicate the presence of many particles on the fibre surface of both fabrics.

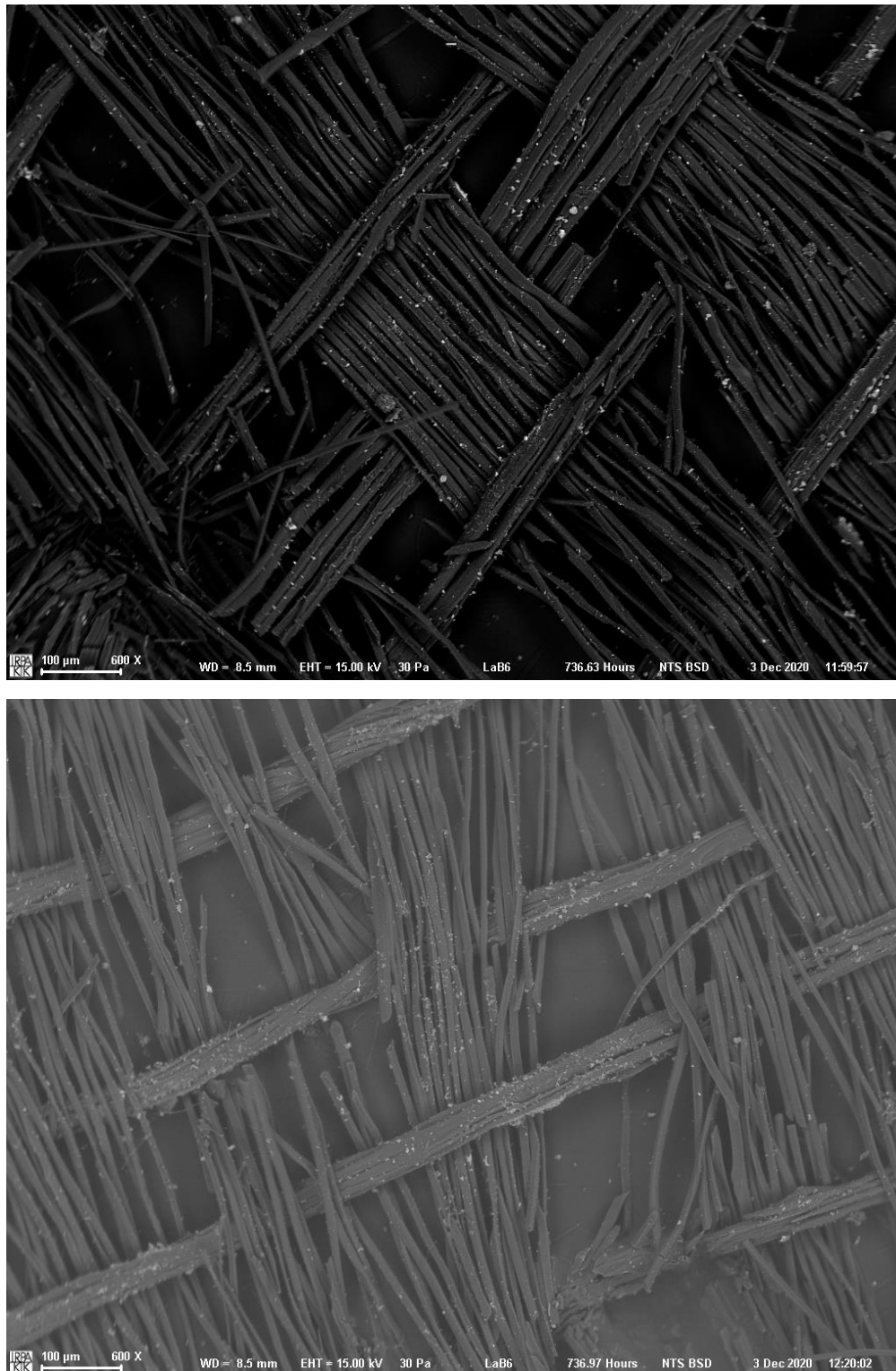


Figure 18: backscattered electron images of the silk fabrics from the dress of the adult on the left, sample 14426a/v01 (top) and the child, sample 14426a/v03 (bottom)

The elemental composition of the filaments and the particles on the surface is analysed with SEM-EDX.

The silk from the dress of the left figure (/v01) contains apart from carbon (C) (partly from the carbon coating) and oxygen (O), a high amount of sulphur (S), calcium (Ca), potassium (K) and silicon (Si). Sodium (Na), aluminium (Al), chlorine (Cl) are detected in low amounts. The beige yarns contain a higher amount of silicon and aluminium than the white yarns. They also contain a trace of iron (Fe) (figure 20).

On the fibre surface, particles are detected containing either a high amount of aluminium (Al), silicon (Si) and potassium (K) or sulphur (S), potassium (K) and calcium (Ca). Small traces of iron are also detected (figure 21).

A scattered pattern of calcium (calcium sulphate) is visible in the SEM-EDX mapping (figure 22).

The silk from the child's dress (/v03) contains in general carbon (C) (partly from the carbon coating) and oxygen (O) and further sulphur (S), calcium (Ca), potassium (K) and sodium (Na), together with small amounts of phosphorus (P) and magnesium (Mg).

Both yarns also contain aluminium (Al) and silicon (Si). However, the amount of these elements is higher in the beige yarn, in which also a low amount of iron (Fe) is detected (figures 23-24).

Surface particles on fibres contain either a high amount of aluminium (Al) and silicon (Si) or sulphur (S), calcium (Ca), and potassium (K) or aluminium (Al) and iron (Fe) (figure 25).

A scattered pattern of calcium and sulphur (calcium sulphate) is visible in the SEM-EDX mapping.

The aluminium and silicon mapping shows the presence of these elements mainly on the beige yarns (figure 26).

The high amount of sulphur, calcium and potassium detected on the fibres, as well as on the particles on the surface of both silk fabrics is striking. It is an indication for a sulphur bleaching treatment, in the late 18th to 20th centuries commonly done by "sulphur stoving", by which sulphurous acid was formed as active bleaching product. This was a process which is very harmful for the silk.

The weighting of the silk might have played a big role in the silk stability as well. Aluminium sulphate and sodium silicates are known products involved in silk weighting procedures in the 19th century, and the presence of iron, especially on the 'beige' warp yarns and some surface particles indicates an iron weighting treatment of the silk fabrics, with increasing acidity as result as a function of degradation (Hacke 2008, Garside et al. 2010).

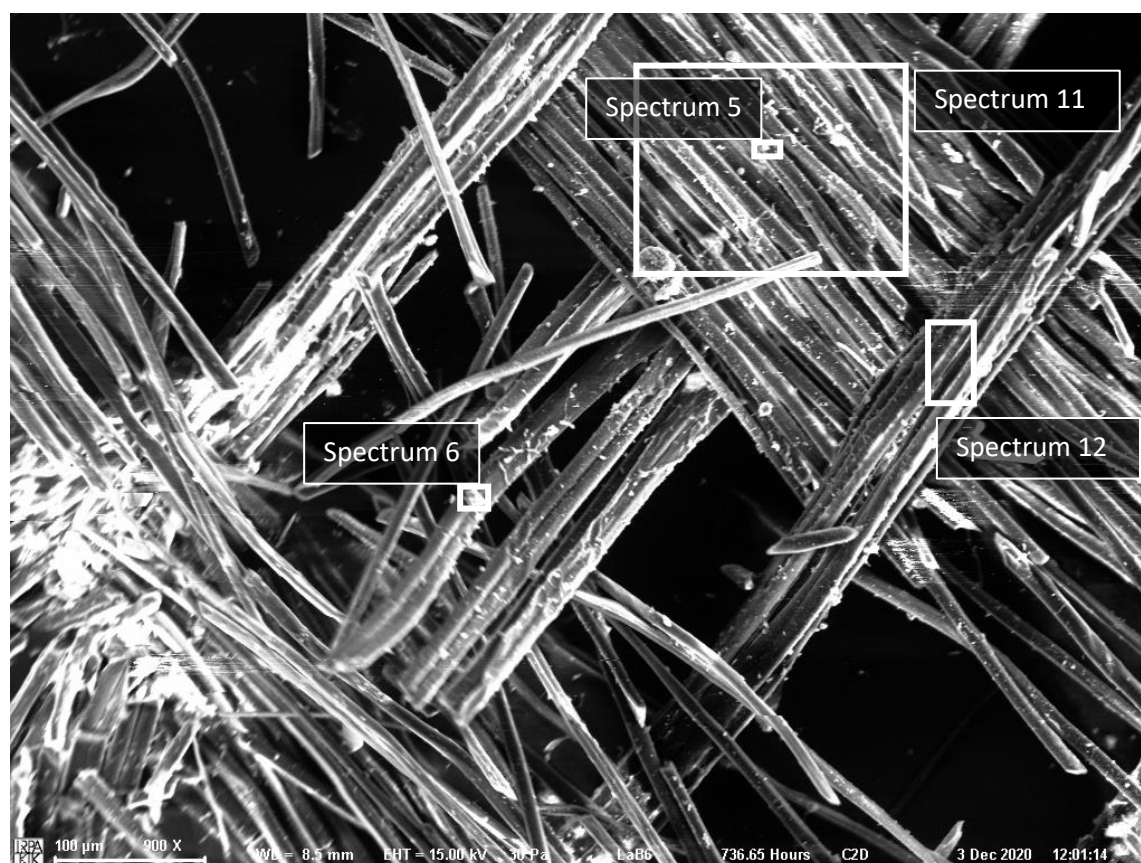


Figure 19: Secondary electron image of sample 14426a/v01 with the indication of the analysed zones in white of the white (spectrum 11) and beige yarns (spectrum 12) and of the surface particles (spectra 5 and 6)

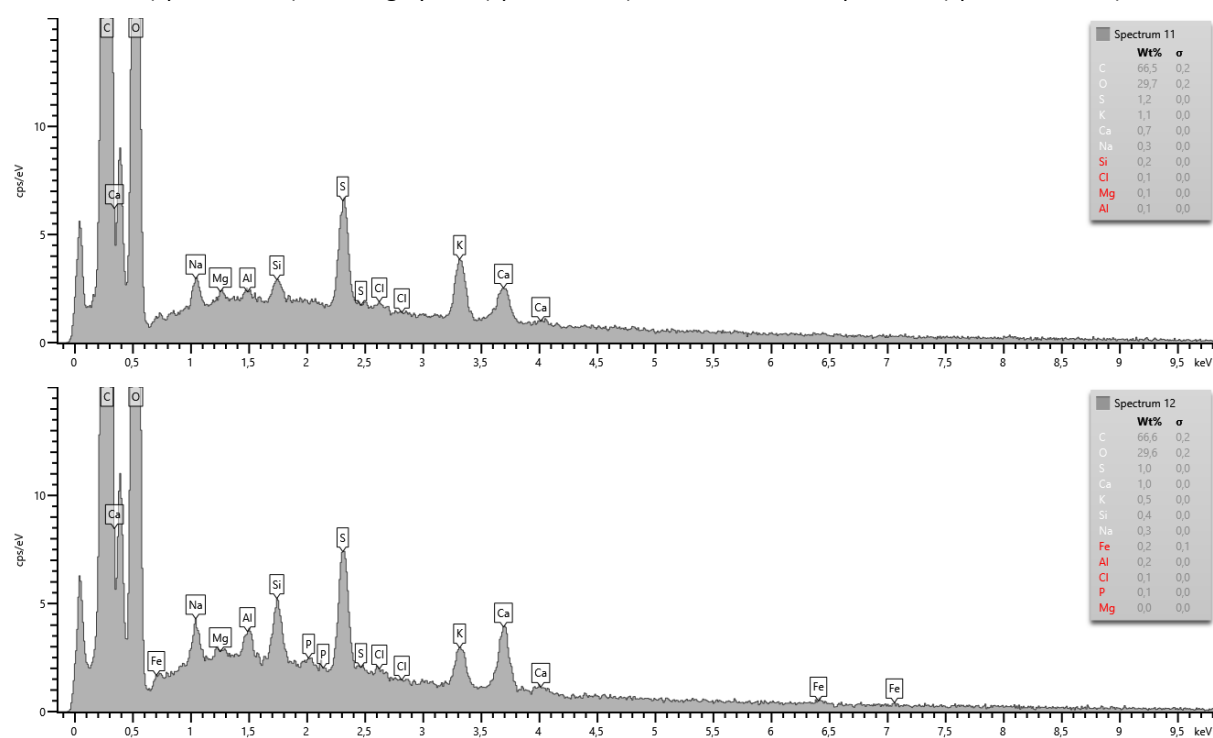


Figure 20: Element spectra of the white yarns (spectrum 11, top) and the beige yarns (spectrum 12, down) of sample 14426a/v01

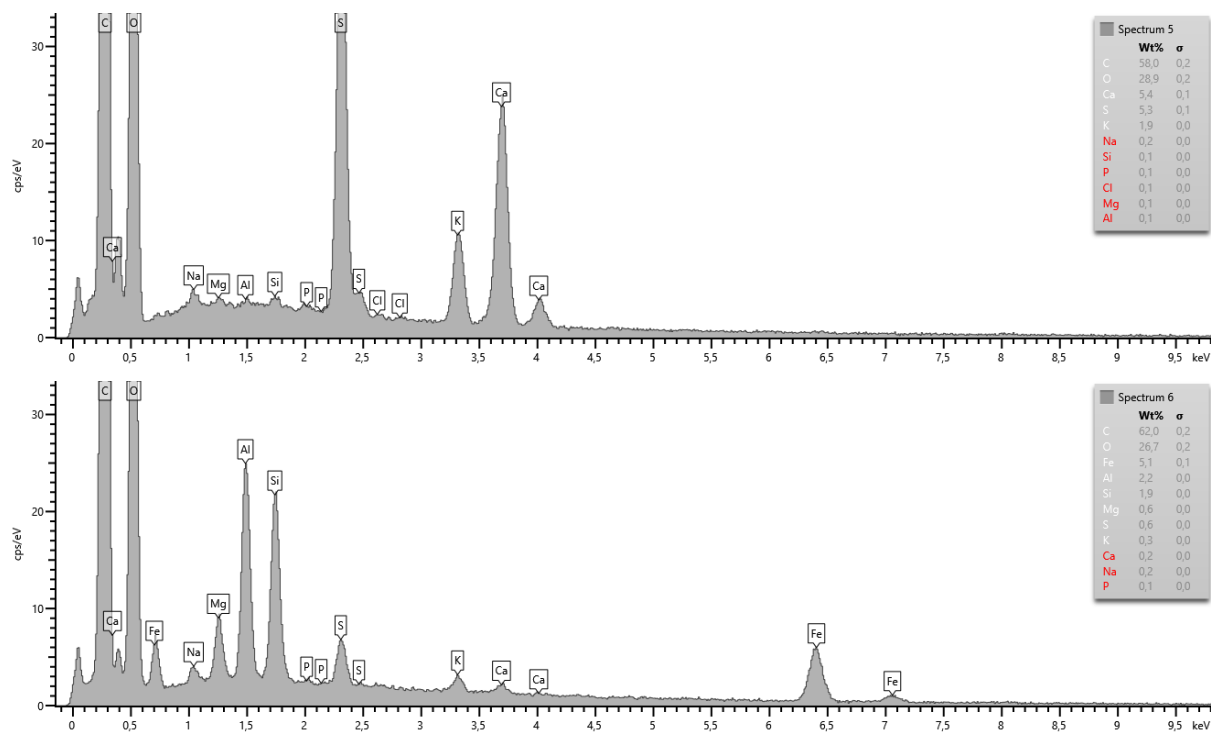


Figure 21: Element spectra of surface particles of sample 14426a/v01 (spectra 5 and 6)

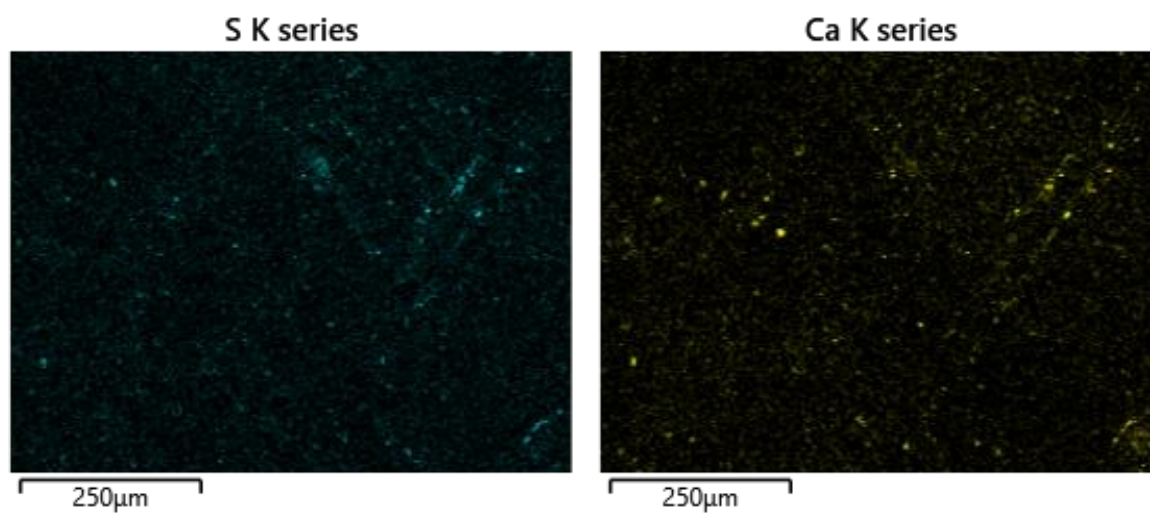


Figure 22: SEM-EDX mapping of sample 14426a/v01 with the partition of sulfur (S) and calcium (Ca)

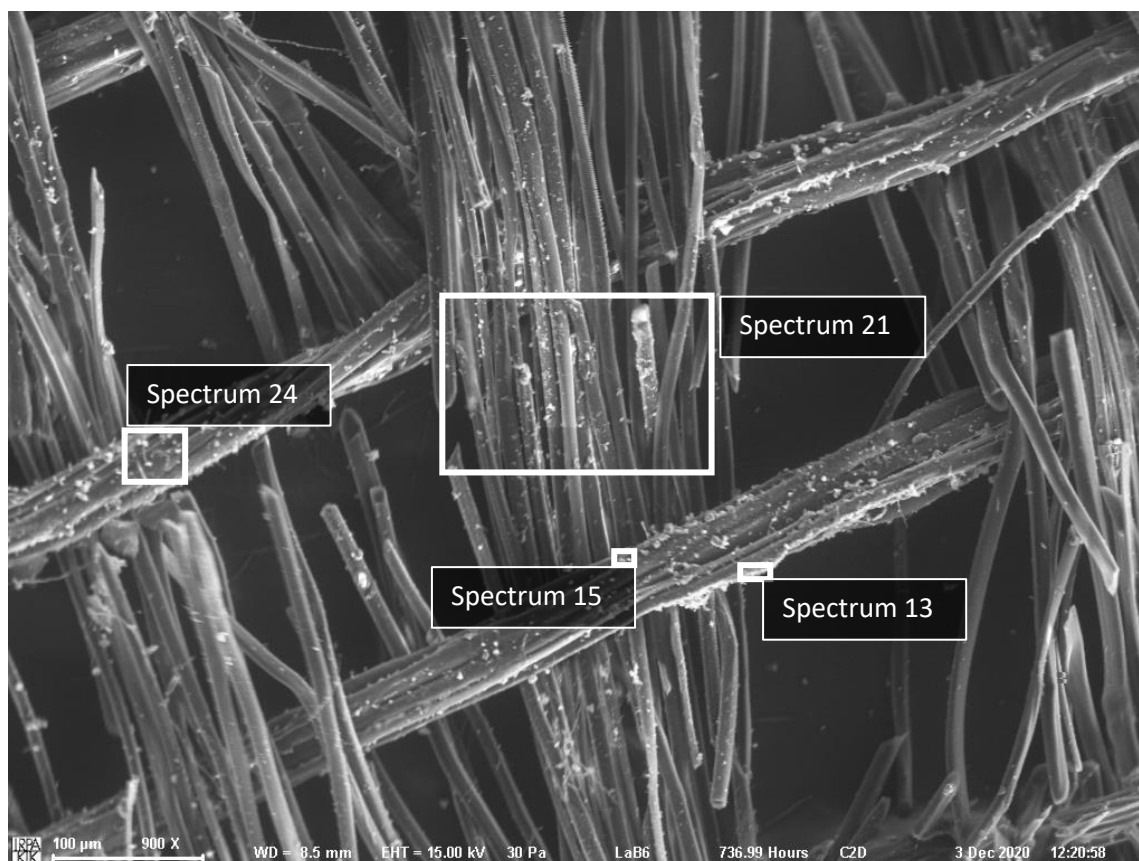


Figure 23: Secondary electron image of sample 14426a/v03 with the indication of the analysed zones in white of the white yarns (spectrum 21) and the beige yarns (spectrum 24)

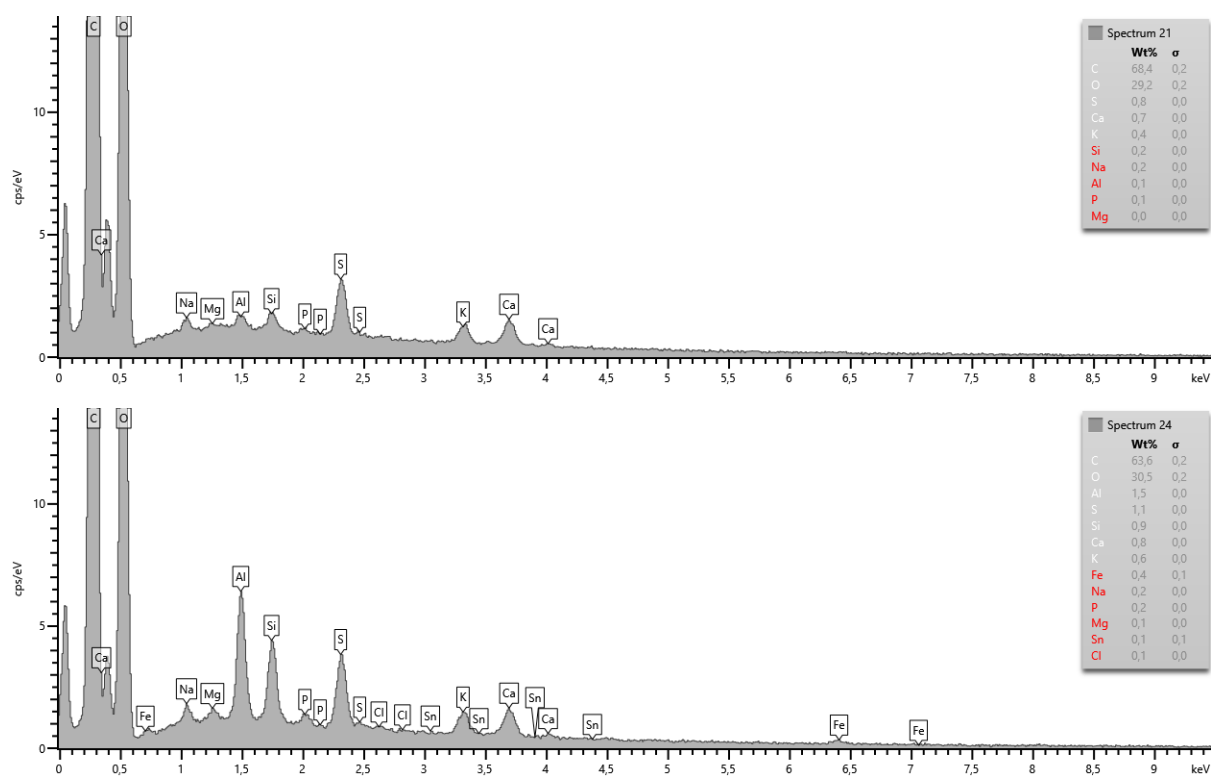


Figure 24: Element spectra of the white yarns (spectrum 21, top) and the beige yarns (spectrum 24, down) of sample 14426a/v03

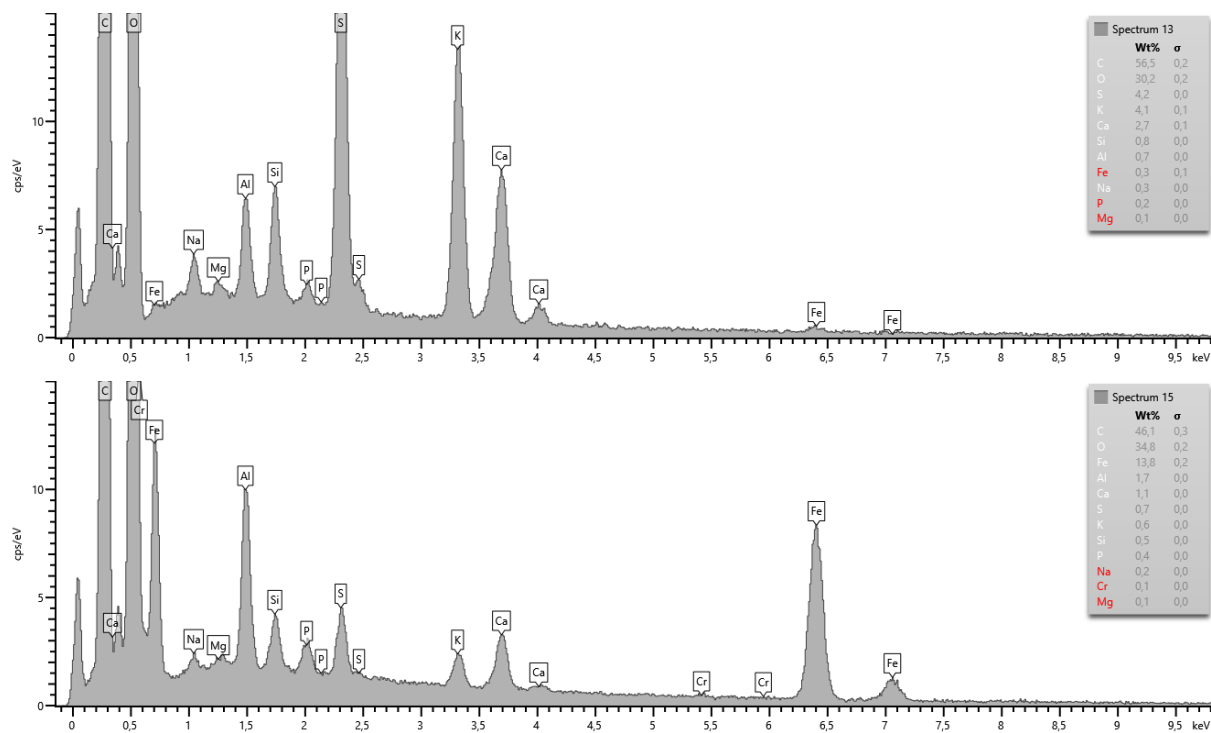


Figure 25: Element spectra of surface particles of sample 14426a/v03 (spectra 13 and 15)

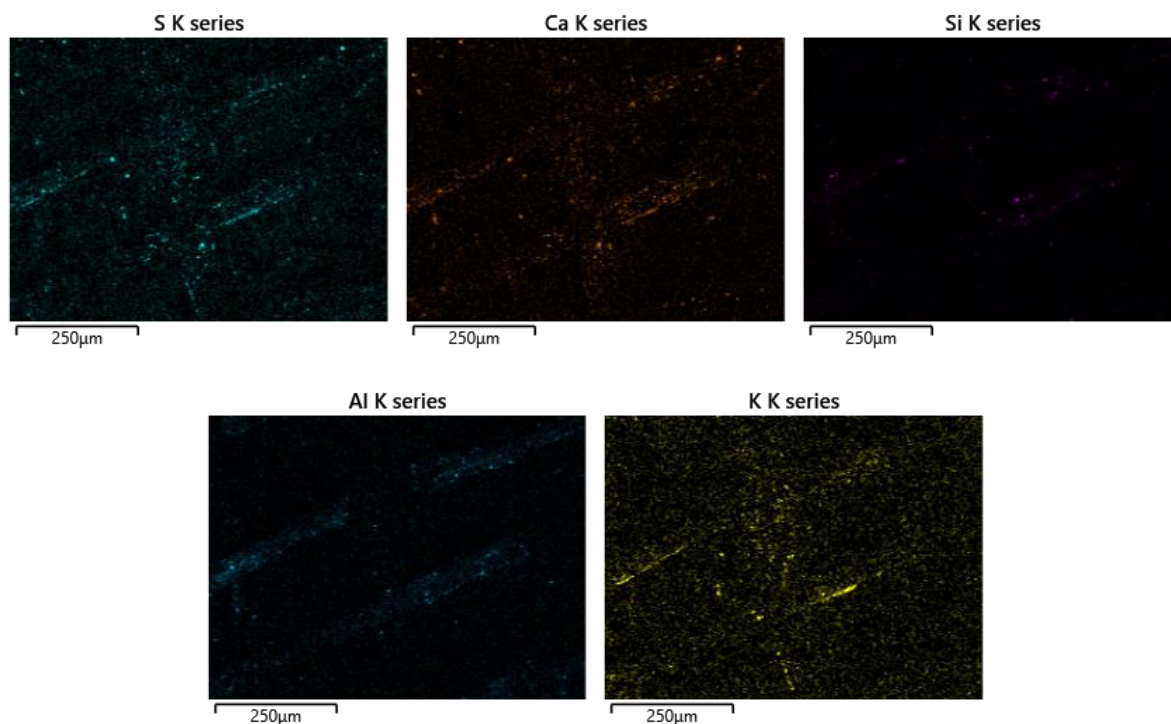


Figure 26: SEM-EDX mapping of the child's dress with the partition of sulphur (S), calcium (Ca), silicon (Si), aluminium (Al), potassium (K)

3. Conclusion

A combination of non-invasive and invasive analyses were performed on these figurines of the holy family.

Hirox images were made to get an overview of the materials used in this object. XRF-analyses identified the nails on the head iron metal nails with a tin solder in the middle. The head itself showed the presence of calcium, FT-IR analyses confirmed the use of calcium sulphate and beeswax. Carbon black and vermilion were used to paint the face. The metal used for the leaves on the breast of the figurines is identified as a copper-zinc alloy (brass). The metal wire on the other hand as copper, with a minor amount of zinc. Lead white was likely present on the textile remains and the white pearl.

Dye analyses of the red yarns of the red/brown fragment identified Mexican cochineal (*Dactylopius coccus* Costa).

As for the beige dresses, Hirox and SEM-EDX images revealed that the extensive degradation was caused by the breaking of threads in both the warp and weft directions while in other places, it is mainly the thicker silk threads without torsion that are the first to break and disappear. These degraded silk fragments are in great contrast to some other areas with much better preserved silk, as from the shawl of the decapitated figure. Both white and beige yarns of the silk of the adult's dress were analysed separately. The samples are very small and brittle, though both yarns are identified as degummed cultivated silk *Bombyx mori* L. No dyes are present in the two silk samples of the dresses.

The backscattered electron images indicate the presence of many particles on the fibre surface of both fabrics. The high amount of sulphur, calcium and potassium detected on the fibres, as well as on the particles on the surface of both silk fabrics are an indication for a sulphur bleaching treatment. In the late 18th to 20th centuries this was commonly done by "sulphur stoving" where sulphurous acid was formed as active bleaching product, which is very harmful for the silk.

The weighting of the silk might have played a big role in the silk stability as well. Aluminium sulphate and sodium silicates are known products involved in silk weighting procedures in the 19th century, and the presence of iron, especially on the 'beige' warp yarns and some surface particles indicates an iron weighting treatment of the silk fabrics, with increasing acidity as result as a function of degradation.

4. References

(1967) Identification of Textile Materials. Published by the Textile Institute, Manchester, 5th edition

Garside, P., Wyeth, P. and Zhang, X. (2010) The inherent acidic characteristics of silk, Part II – Weighted silks. *e-Preservation Science* 7, 126-131.

Garside, P. Mills, G., Smith, J. and Wyeth, P. (2014) An investigation of weighted and degraded silks by complementary microscopy techniques. *e-Preservation Science* 11, 15-21.

Hacke, M. (2008) Weighted silk: history, analysis and conservation. *Reviews in conservation* 9, 3-15.

Haugan, E. and Holst, B. (2013) Determining the fibrillar orientation of bast fibres with polarized light microscopy: the modified Herzog test (red plate test) explained. *Journal of microscopy* 252 (2), 159-168.

Kshirsagar, S. V., Singh, B., Fulari, S. P. (2009) Comparative study of human and animal hair in relation with diameter and medullary index, *Indian Journal of forensic Medicine and Pathology* Vol.2 N°3, 105-108

Petraco, N. en Kubic, T. (2004) Colour atlas and manual of microscopy for criminalists, chemists and conservators, CRC press, 69-75

Van Bos M., Watteeuw L., “Composition of iron gall inks in Illuminated Manuscripts (11th -16th century). The Use by Scribes and Illuminators”, in: *Care and conservation of Manuscripts*, eds. Gillian Fellows-Jensen and Peter Springborg, The Arnamagnæan Institute, University of Copenhagen, Museum Tusculanum Press, 2014: 365 – 381

Vanden Berghe, I., Gleba, M. and Mannering, U. (2009) Towards the identification of dyestuffs in Early Iron Age Scandinavian peat bog textiles. *Journal of Archaeological Science* 36, 1910-1921

Vanden Berghe, I. (2016) The identification of Cochineal Species in Turkmen Weavings; A Special Challenge in the Field of Dye Analysis. In *Turkmen Carpets. A New Perspective*, volume I. Eds. Jürg Rageth and ‘Freunde des Orientteppiche Basel’, Abächerli Media AG, Sarnen (Switzerland), 303-310

Vanden Berghe, I., Vandenbergh, M. and Coudray, A. (2020) KIK-IRPA (non-commercial) fibre reference database

Von Bergen, W. and Krauss, W. (1945) *Textile Fibre Atlas*, a collection of photomicrographs of old and new textile fibres. Textile book publisher Inc., New York (second printing)

Watteeuw L., Van Bos M. “A 15th-century Flemish enclosed garden in cuir bouilli. Production, degradation and conservation issues of a small painting on leather”. In *ICOM-CC 17th Triennial Conference Preprints*, Melbourne, 15–19 September 2014